THE JOURNAL OF BIOLOGICAL CHEMISTRY VOL. 284, NO. 23, pp. 15692–15700, June 5, 2009

Dual Regulation of Muscle Glycogen Synthase during Exercise by Activation and Compartmentalization*

Received for publication, February 5, 2009, and in revised form, March 30, 2009 Published, JBC Papers in Press, April 1, 2009, DOI 10.1074/jbc.M900845200

Clara Prats[‡1], Jørn W. Helge[‡], Pernille Nordby[‡], Klaus Qvortrup[‡], Thorkil Ploug[‡], Flemming Dela[‡], and Jørgen F. P. Wojtaszewski[§2]

From the [‡]Copenhagen Muscle Research Center, Center for Healthy Ageing, Department of Biomedical Sciences, and [§]Molecular Physiology Group, Institute of Exercise and Sport Sciences, University of Copenhagen, DK-2200 Copenhagen N, Denmark

Glycogen synthase (GS) is considered the rate-limiting enzyme in glycogenesis but still today there is a lack of understanding on its regulation. We have previously shown phosphorylation-dependent GS intracellular redistribution at the start of glycogen re-synthesis in rabbit skeletal muscle (Prats, C., Cadefau, J. A., Cussó, R., Qvortrup, K., Nielsen, J. N., Wojtaszewki, J. F., Wojtaszewki, J. F., Hardie, D. G., Stewart, G., Hansen, B. F., and Ploug, T. (2005) *J. Biol. Chem.* 280, 23165–23172). In the present study we investigate the regulation of human muscle GS activity by glycogen, exercise, and insulin. Using immunocytochemistry we investigate the existence and relevance of GS intracellular compartmentalization during exercise and during glycogen re-synthesis. The results show that GS intrinsic activity is strongly dependent on glycogen levels and that such regulation involves associated dephosphorylation at sites 2+2a, 3a, and 3a + 3b. Furthermore, we report the existence of several glycogen metabolism regulatory mechanisms based on GS intracellular compartmentalization. After exhausting exercise, epinephrine-induced protein kinase A activation leads to GS site 1b phosphorylation targeting the enzyme to intramyofibrillar glycogen particles, which are preferentially used during muscle contraction. On the other hand, when phosphorylated at sites 2+2a, GS is preferentially associated with subsarcolemmal and intermyofibrillar glycogen particles. Finally, we verify the existence in human vastus lateralis muscle of the previously reported mechanism of glycogen metabolism regulation in rabbit tibialis anterior muscle. After overnight low muscle glycogen level and/or in response to exhausting exercise-induced glycogenolysis, GS is associated with spherical structures at the I-band of sarcomeres.

The desire to understand metabolism and its regulation dates back several centuries, but it has exponentially increased during the last decades in an effort to treat or prevent type 2 diabetes mellitus (T2DM).[3] Defective muscle glycogen synthesis has been repeatedly reported in patients with T2DM (1–3). Several studies have shown impairments of insulin-induced glycogen synthase (GS) activation in skeletal muscle from T2DM patients and in healthy subjects at increased risk for T2DM, such as healthy obese and first-degree relatives of patients with T2DM (4–9).

The first scientific studies on GS date from the 1960s, but still today there is a lack of understanding on its regulation. GS is the rate-limiting enzyme in glycogenesis and is classically used as an example of an allosterically and covalently regulated enzyme. It is well accepted that GS is complexly regulated by sequences of hierarchal phosphorylations (10) in at least nine sites and by its allosteric activator, glucose 6-phosphate (G6P) (11, 12). However, the exact effects of GS phosphorylation at different sites on its regulation are still not clear. GS phosphorylation sites are distributed between the NH_2- and the COOH-terminal domains. The NH_2 terminus domain contains two sites, 2 (Ser^7) and 2a (Ser^{10}), that are phosphorylated in a hierarchal mode. Phosphorylation of site 2 is needed as a recognition motif for casein kinase 1 to phosphorylate site 2a (13, 14). Several protein kinases have been reported to phosphorylate site 2 *in vitro*, among them PKA, CaMKII, PKC, AMPK, GPhK, and MAPKAPKII (15–17). At the COOH terminus of muscle GS, there are at least seven phosphorylation sites; sites 3a (Ser^{640}), 3b (Ser^{644}), 3c (Ser^{648}), 4 (Ser^{652}), 5 (Ser^{656}), 1a (Ser^{697}), and 1b (Ser^{710}). Sites 3, 4, and 5 are phosphorylated in a hierarchal mode. Casein kinase II phosphorylates site 5, establishing a recognition motif for GSK-3 to phosphorylate sequentially sites 4, 3c, 3b, and 3a (18–21). Dephosphorylation of sites 2 and 3 increase GS intrinsic activity much more than dephosphorylation of the remaining sites, which have little or no effect on the enzyme activity (22). The effect of GS phosphorylation at sites 1a and 1b remains elusive. G6P binding reverses covalent inactivation of GS by phosphorylation (11) and increases susceptibility of the enzyme to be activated by the action of protein phosphatases (23), mainly by glycogen-targeted protein phosphatase 1.

Intracellular compartmentalization of GS has been reported in several studies. In isolated hepatocytes, incubation with glucose induces GS activation and intracellular translocation to

* This work was supported in part by The Copenhagen Muscle Research Centre, the Novo Nordisk Research Foundation, The Danish Diabetes Association, the Lundbeck Foundation, the Velux Foundation, the Foundation of 1870, Direktør Jacob and Olga Madsens Foundation, Aase and Ejnar Danielsens foundation, and an Integrated Project (Grant LSHM-CT-2004-005272) funded by the European Commission and The Danish Medical Research Council.

[1] To whom correspondence should be addressed: Blegdamsvej 3, 2200 Copenhagen N, Denmark. Tel.: 45-3532-7423; Fax: 45-3532-7555; E-mail: cprats@mfi.ku.dk.

[2] Supported by a Hallas Møller Fellowship from The Novo Nordisk Foundation.

[3] The abbreviations used are: T2DM, type 2 diabetes mellitus; GS, glycogen synthase; G6P, glucose 6-phosphate; PKA, protein kinase A; VL, vastus lateralis; FV, fractional velocity; glc, glucose; CHO, carbohydrate; GSI, glycogen synthase glucose 6-phosphate-independent form.

the cell periphery (24). In contrast, in the absence of glucose, GS has been shown to be mainly located inside the nucleus of both cultured liver and muscle cells; however, following addition of glucose GS translocates to the cytosol (25). In a previous study, we reported a novel regulatory mechanism of skeletal muscle glycogen metabolism (26). We showed that severe glycogen depletion induced by muscle contraction leads to rearrangement of cytoskeleton actin filaments to form dynamic intracellular compartments. Both GS and phosphorylase associate with such compartments to start glycogen re-synthesis. Furthermore, we showed that GS phosphorylated at site 1b (P-GS1b) was located at the cross-striations, the I-band of sarcomeres, whereas when phosphorylated at sites 2+2a (P-GS2+2a), GS formed some clusters homogeneously distributed along muscle fibers. In the present study we investigate the existence and relevance of such regulatory mechanism in human muscle metabolism.

EXPERIMENTAL PROCEDURES

Ten healthy young well trained male subjects (age 26 ± 1 years, body mass index of 24.4 ± 0.7 kg · m^{-2} and VO_{2max} of 57 ± 2 ml of O_2 · (min · kg)$^{-1}$ were included in the study; all subjects gave verbal and written consent to participate. The study was approved by the ethical committee of Copenhagen and Frederiksberg municipality (01-257174) and adhered to the Helsinki Declaration.

The experiment was performed on two consecutive days. On day 1 a leg was randomly appointed as the glycogen pre-depleted leg, and this leg completed a glycogen depletion exercise protocol using a knee extension ergometer (27). The protocol consisted of a 30-min warm-up exercise (50% W_{max}) followed by a total of 39 consecutive 3-min intervals of kicking at maximal sustainable workload. Between each working interval, subjects were allowed to rest for 2 min by kicking at 0% W_{max}. When unable to complete the working interval, the workload was lowered 5%. Afterward subjects performed 1 h of arm cranking at 75% of maximal heart rate using an Angio arm ergometer (Lode BV, Groningen, The Netherlands) to decrease upper-body muscles and liver glycogen stores. Thereafter, subjects went home and were only allowed to eat 6500 kJ of a standardized meal containing 25% energy (*E*%) protein, 5 *E*% carbohydrate, and 70 *E*% fat until the next day. On day 2, the subjects returned overnight fasted, muscle biopsies were obtained from vastus lateralis (VL) muscle, as previously described (28). Next, subjects initiated an exhausting exercise protocol, which started as a two-leg knee extensor exercise at 85% of W_{max}. Blood samples were collected every 30 min until and at exhaustion. After 60 min of exercise the workload was increased to 90% W_{max}, after 90 min to 95% W_{max}, after 105 min to 100% W_{max}, and after 120 min to 105% W_{max} until exhaustion. At exhaustion of the first leg, exercise was stopped and a muscle biopsy was obtained, after that the unexhausted leg kept on kicking until exhaustion, when a biopsy from the second exhausted VL muscle was taken. All subjects but one exhausted the pre-depleted leg before the control leg. Subjects were then moved to a bed where they ingested 1 g of glucose per kilogram of body mass dissolved in 500 ml of water. After 30 min of rest, a muscle biopsy was obtained from the pre-depleted leg and, immediately after, subjects consumed a high glycemic index sandwich (1 g of glucose per kilogram of body mass). After 120 min of rest a final pre-depleted muscle biopsy was obtained. Throughout the experiment, subjects were allowed unlimited access to water and were encouraged to drink.

Analyses of Blood Plasma Substrate and Hormones—Blood for determination of plasma glucose were analyzed using conventional commercially available assays on an automatic analyzer (Hitachi, 612 Automatic Analyzer, and Roche Applied Science). Plasma insulin concentrations were determined by a commercial enzyme-linked immunosorbent assay (DakoCytomation, Great Britain). Arterial plasma epinephrine concentrations were determined by a commercial radioimmunoassay (High Sensitive 2 CAT RIA, Labor Diagnostika, Nord, Germany).

Processing of Muscle Biopsies—After the biopsies were excised the tissue was carefully dissected and a fraction was rapidly frozen in liquid nitrogen, whereas a second fraction was immersed in cold Krebs-Henseleit bicarbonate buffer containing procaine hydrochloride (1 g/liter) for 5 min and either fixed for light or electron microscopy analysis (29, 30).

Muscle Glycogen—Muscle glycogen was measured as previously described (31).

Muscle GS Activity—Muscle GS activity was measured in triplicates using a 96-well plate assay (Unifilter 350 Plates, Whatman, Cambridge, UK) (36). GS activity was determined in the presence of 8, 0.17, or 0.02 mM G6P and reported as %GSI (100 × [activity (0.02 mM G6P)/activity (8 mM G6P)]) or as %FV (100 × [activity (0.17 mM G6P)/activity (8 mM G6P)]).

SDS-PAGE and Western Blotting—Muscle proteins were separated using 7.5% Tris-HCl gels (Bio-Rad, Denmark), and transferred (semi-dry) to polyvinylidene difluoride membranes (Immobilon Transfer Membrane, Millipore A/S, Denmark) (32). Primary antibodies used for Western blotting: Anti-GS was a polyclonal rabbit antibody (32). For detection of P-GS3a+3b, P-GS2, P-GS2+2a, P-GS1a, and P-GS1b, antibodies were raised against different peptides as described (26, 33). The specificity of these antibodies has previously been reported (33). The antibody against P-GS3a was purchased from Cell Signaling.

Fluorescence Immunohistochemistry in Single Muscle Fibers—This was performed as previously described (26). Total GS was immunodetected using a rabbit polyclonal antibody (Abcam) or a rabbit antibody raised against a synthetic peptide containing the last nine monoacids from human muscle GS: ^{729}TSSLGEERN^{737} (A gift from Prof. Joan J. Ginovart). GS phosphorylated at sites 1a, 1b, 2, 2+2a, or 3a+3b were immunodetected using the same phospho-specific antibodies as for Western blotting. Secondary antibodies conjugated with Alexa 488 or Alexa 568 (Invitrogen) were used. All antibodies were diluted in 50 mM glycine, 0.25% bovine serum albumin, 0.03% saponin, and 0.05% sodium azide in phosphate-buffered saline. Between incubation periods, muscle fibers were washed with the same buffer, but the last wash was performed with phosphate-buffered saline. Negative controls for each of the staining conditions were performed by staining without primary antibody or without primary and secondary antibodies. Muscle fibers were mounted in Vectashield mounting medium and analyzed. Confocal images were collected with a TCS SP2 microscope (Leica)

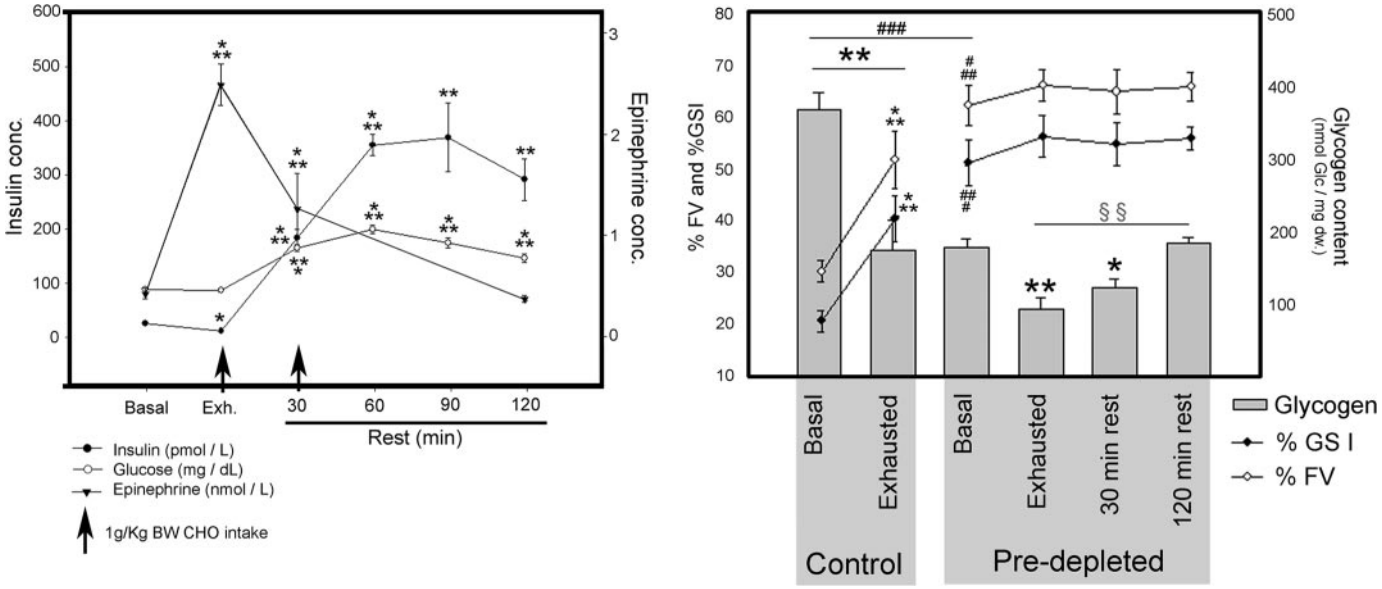

FIGURE 1. **Plasma glucose and hormones.** Blood samples were taken every 30 min during the intervention. Vastus lateralis biopsies from nine subjects were taken before (*Basal*) and after exhausting exercise (*Exhausted*) from both Control and Pre-depleted legs. Afterward, subjects ingested 1g of glucose per kilogram body weight and rested for 30 min. Biopsies were taken and subjects ingested another gram of glucose per kilogram body weight. Last biopsies were taken 2 h after the end of exhausting exercise. *Left*, plasma glucose, insulin, and epinephrine concentrations were measured before and at 0, 30, 60, 90, and 120 min after exhausting exercise. *Arrows* indicate the intake of 1 g of glucose per kilogram body weight. Results are expressed as means ± S.E. ($n = 9$). Basal plasma glucose values are 4.85 ± 0.073 mmol·liter^{-1}, 4.32 ± 0.17 mmol·liter^{-1} at exhaustion, 9.10 ± 0.33 mmol·liter^{-1} after 30 min rest, 11.03 ± 0.462 mmol·liter^{-1} after 60-min rest, 9.64 ± 0.53 mmol·liter^{-1} after 90-min rest, and 8.05 ± 0.417 mmol·liter^{-1} after 2-h rest. *Right*, glycogen content, percentage of GS fractional activity (%FV) and percentage of GS I form (%GSI) were measured as described under "Experimental Procedures." Results are expressed as mean ± S.E. Statistical significance was assessed by one-way analysis of variance and is represented as *, $p < 0.05$; **, $p < 0.01$; and ***, $p < 0.005$ *versus* basal; ###, $p < 0.005$ between basal; and §§, $p < 0.01$ exhausted *versus* rested.

using a Plan-Apo ×63/1.32 oil objective at 20 °C. Imaging settings were set so that no signal was detected in the respective negative controls and a low fraction of pixels showed saturation intensity values. Confocal z-stack images were collected from the surface to the center of muscle fibers, spaced 0.35 μm apart in the z-plane. Projections of four z-planes were constructed and analyzed using Metamorph software (Universal Imaging Corp.).

Transmission Electron Microscopy—To perform immunogold labeling of P-GS1b or P-GS2+2a, single muscle fibers were isolated, and immunohistochemistry was performed as described above. Secondary antibodies conjugated to nanogold particles (Nanoprobes) were used. After the final wash single muscle fibers were fixed with 2% glutaraldehyde for 1 h, washed 3 × 5 min with 0.1 M Sorensen buffer (pH 7.4) (34) and 3 × 5 min with milliQ H_2O. Silver enhancement (Nanoprobes) was performed, and muscle fibers were postfixed with 1% osmium in 0.1 M Sorensen buffer (pH 7.4) for 20 min. Muscle fibers were then dehydrated in a graded series of ethanol, transferred to propylene oxide, and embedded in Epon according to standard procedures. Ultrathin sections were cut with a Reichert-Jung Ultracut E microtome and collected on one-hole copper grids with Formvar supporting membranes. Sections were stained with uranyl acetate and lead citrate and examined with a Phillips CM 100 transmission electron microscope operated at an accelerating voltage of 80 kV. Images were collected using a Megaview 2 camera and processed with the Analysis software package.

Statistic Analysis—The data were analyzed using SigmaStat software. Results are expressed as means ± S.E. A one-way analysis of variance test was used to assess statistical significance of the difference between groups. The linear dependence between different groups of data was assessed by the Pearson product-moment correlation coefficient.

RESULTS

Ten healthy young subjects performed a glycogen depletion exercise protocol with one leg, the pre-depleted leg. Liver and upper-body muscle glycogen storages were also depleted by using an arm cranking exercise protocol. Subjects went home and were only allowed to eat a low carbohydrate meal. Next day, subjects were asked to perform an exhausting exercise with both legs. Subjects were then given a high glucose drink at the end of the exhausting exercise and a high CHO sandwich after 30 min rest.

Plasma Glucose and Hormones—Blood samples were collected before and after exhausting exercise and after 30, 60, 90 and 120 min of rest. Glucose, insulin and epinephrine blood concentrations were measured (Fig. 1, *left panel*). During exhausting exercise, epinephrine increased from 0.43 ± 0.05 to 2.55 ± 0.21 nmol·liter^{-1}, and gradually reversed to basal levels after 120 min rest. Glucose levels remained constant during exhausting exercise. Insulin decreased from 23.2 ± 2.0 to 9.8 ± 1.3 pmol·liter^{-1} ($p < 0.05$) during exhausting exercise. Thirty minutes after the ingestion of glucose drink, glucose and insulin levels increased to 9.1 ± 0.33 mmol·liter^{-1} ($p < 0.001$) and 183.5 ± 15.2 pmol·liter^{-1} ($p < 0.0001$), respectively. At this point subjects were asked to eat a high CHO sandwich. Thirty minutes later, glucose levels had further increased to 11.0 ± 0.46 mmol·liter^{-1}, while plasma insulin concentration had

increased to 355.7 ± 19.2 pmol·liter^{-1}, remaining both significantly increased after 120 min of rest (Fig. 1, *left panel*).

Muscle Glycogen Content—VL muscle biopsies from both legs were obtained before and after exhausting exercise, 30 min after the ingestion of the glucose drink and 90 min after the ingestion of the high CHO sandwich biopsies were taken from the pre-depleted muscle. Before starting the exhausting exercise, glycogen content in VL muscle was significantly lower in the pre-depleted compared with the control muscle, 180.0 ± 12.3 and 370.0 ± 24.4 nmol glc·(mg dry weight)$^{-1}$ ($p < 0.0005$), respectively (Fig. 1, *right panel*). After exhausting exercise, glycogen levels further decreased 54 and 47% in control and pre-depleted muscle, respectively. Glycogen content in exhausted pre-depleted muscle was 75% lower than in basal control ($p < 0.0005$). After 30 min of rest, glycogen levels had increased from 95 ± 14.3 to 124.5 ± 12.5 nmol glc·(mg dry weight)$^{-1}$, but a statistically significant glycogen re-synthesis (185.0 ± 8.8 nmol glc·(mg dry weight)$^{-1}$) was first detected after 120 min rest (Fig. 1, *right panel*).

GS Activity and Phosphorylation after Exhausting Exercise and at the Start of Glycogen Re-synthesis—GS activity was measured in the presence of 8 mM, 0.17 mM, and 0.02 mM G6P. From these, the percentage of fractional velocity (%FV) and of GSI form (%GSI) were calculated. In control muscle, GS was activated by exercise detected both as increased %FV (from 30.2 ± 2.9 to 51.8 ± 5.5% ($p < 0.005$)) and %GSI (from 20.6 ± 2.0 to 40.4 ± 4.4% ($p < 0.005$)) (Fig. 1, *right panel*). Before exhausting exercise, pre-depleted muscle had markedly higher GS activity compared with control muscle, with 62.3 ± 3.8%FV and 51.2 ± 4.4%GSI, respectively (Fig. 1, *right panel*).

No significant changes in total GS protein or phosphorylation at sites 1a and 2 were detected at any of the studied time points (Fig. 2). After exhausting exercise of control muscle, GS phosphorylation at site 1b significantly increased ($p < 0.05$), while phosphorylation at site 3a decreased ($p < 0.01$) (Fig. 2). Before the start of the exhausting exercise, GS phosphorylation at sites 2+2a, 3a, and 3a+3b was significantly lower in the pre-depleted muscle compared with the controls. As in the controls, exhausting exercise of pre-depleted muscle also lead to increased GS phosphorylation at site 1b ($p < 0.05$). Note that, even though the glycogen level in basal pre-depleted muscle was 51% lower than in basal controls (Fig. 1, *right panel*) in both groups exhausting exercise induced a similar increase in GS phosphorylation at site 1b. In addition, exhausting exercise of pre-depleted muscle induced a further 40% decrease in GS phosphorylation at GS site 3a+3b ($p < 0.05$).

GS Intrinsic Activity Is Dependent on Phosphorylation State at Sites 3a, 3b, 2, and 2a, Which in Turn Are Highly Dependent on Muscle Glycogen Content—Analysis of the interdependency between GS activation state and glycogen content (Fig. 3*A*), shows a clear strong inverse correlation between %FV and glycogen content ($p < 0.0001$) and between %GSI and glycogen content ($p < 0.0001$). GS activity in the presence of 8 mM G6P is considered the total enzyme activity, whereas in the presence of 0.17 mM only intermediate phosphorylated forms and completely dephosphorylated forms of GS contributed to activity. In the presence of 0.02 mM G6P only highly dephosphorylated forms of GS were active. The results show that GS activity in the presence of 0.17 or 0.02 mM G6P was highly dependent on the

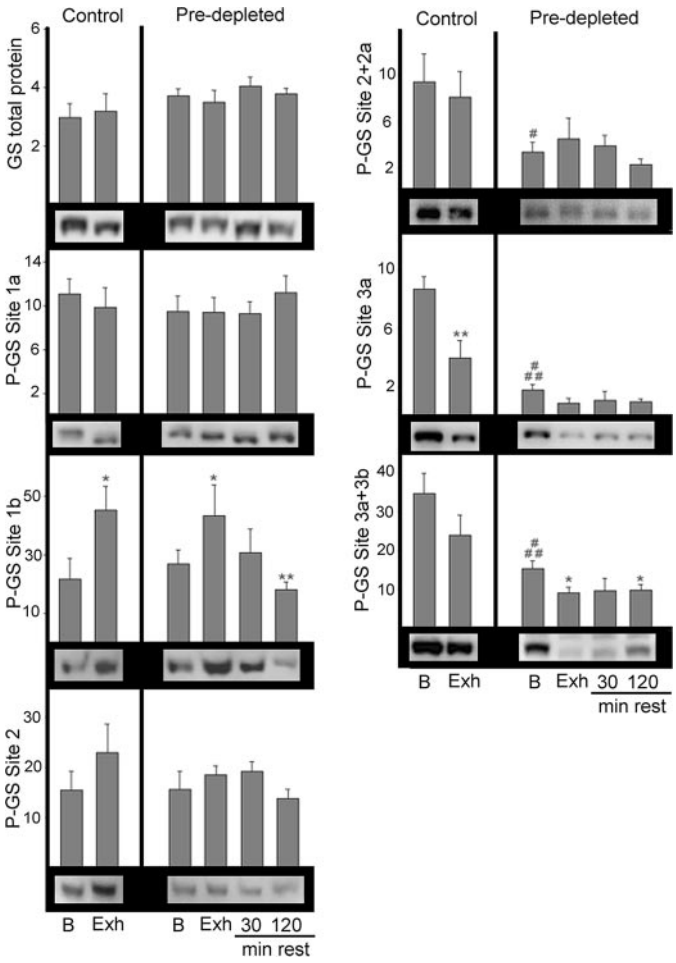

FIGURE 2. **Western blot analysis of GS phosphorylation at sites 1a, 1b, 2, 2+2a, 3a, and 3a+3b.** Muscle homogenates from vastus lateralis anterior muscle from nine subjects were used to quantify phosphorylation of GS at different sites by Western blot using phosphospecific antibodies. Total GS was measured as a control. Representative gels are shown. Results are expressed as arbitrary density units, mean ± S.E. Statistical significance was assessed by one-way analysis of variance and is represented as *, $p < 0.05$ and **, $p < 0.01$ *versus* basal and #, $p < 0.05$ and ###, $p < 0.005$ between basals.

phosphorylation state at sites 2+2a, 3a, and 3a+3b (Fig. 3*B*, $p < 0.0001$). Furthermore, analysis of the interdependency between GS phosphorylation at the different sites and muscle glycogen content (Fig. 3*C*) shows a strong positive correlation between glycogen levels and GS phosphorylation at sites 2+2a, 3a, and 3a+3b. A three-dimensional graph plotting glycogen content *versus* phosphorylation at sites 2+2a and 3a+3b displays the strong direct and linear interdependency between the three variables (Fig. 3*D*).

Phosphorylation-dependent GS Intracellular Distribution in Human Skeletal Muscle—Phospho-specific antibodies against GS sites 1b, 1a, 2, 2+2a, 3a, and 3a+3b were used to investigate their intracellular distribution in human VL muscle. When phosphorylated at sites 1a, 2, 3a, or/and 3a+3b, GS was found in several intracellular regions, as the total GS distribution, showing a striated and a dotted pattern of distribution and associated with some cellular compartment found at the perinuclear regions (Fig. 4, *top panel*). In contrast, P-GS1b is specifically found at the muscle striations, while P-GS2+2a presents a dotted pattern of distribution, forming cluster-like structures

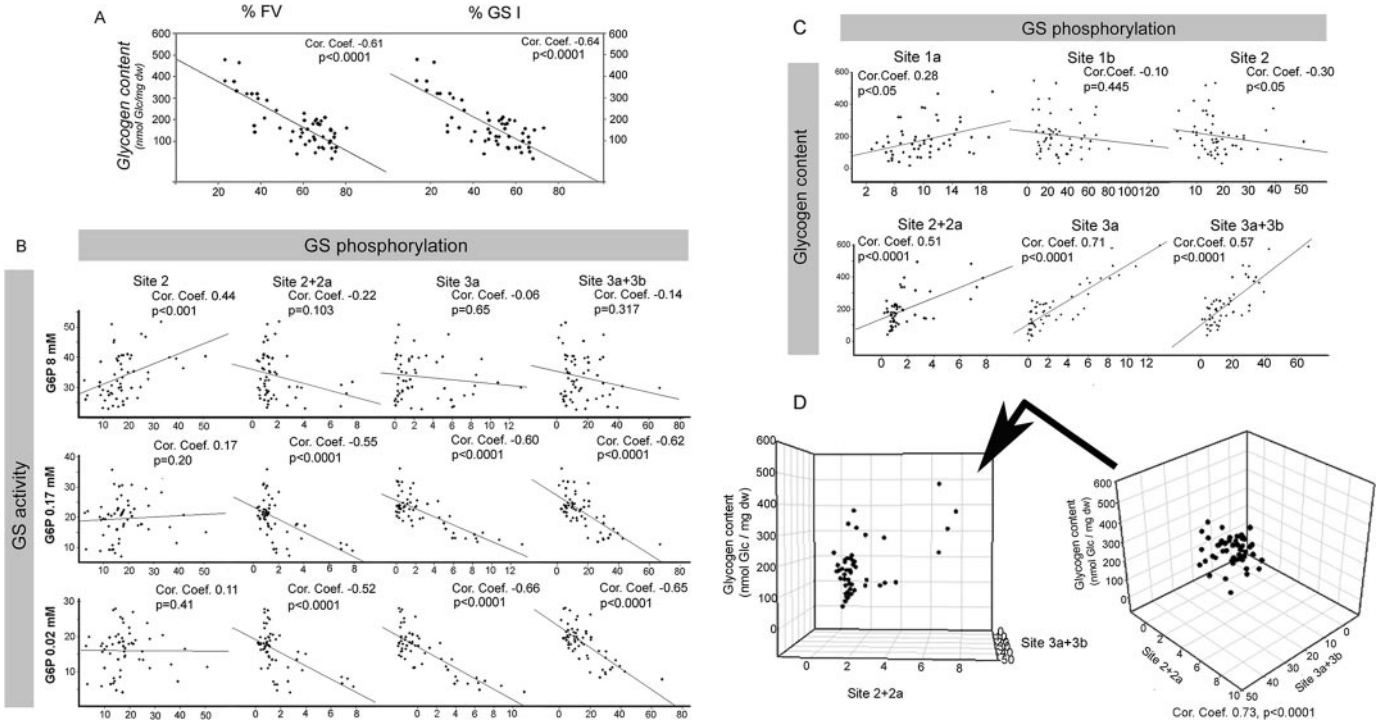

FIGURE 3. **Regulation of GS intrinsic activity by glycogen content and phosphorylation at sites 2+2a and 3a+3b.** *A*, glycogen content is plotted *versus* GS intrinsic activity, %FV and %GSI. *B*, GS activity in the presence of 8 mM, 0.17 mM, or 0.02 mM G6P is plotted *versus* GS phosphorylation at sites 2, 2+2a, 3a, and 3a+3b. *C*, glycogen content is plotted *versus* GS phosphorylation at sites 1a, 1b, 2, 2+2a, 3a, and 3a+3b. *D*, three-dimensional plot of glycogen content *versus* GS phosphorylation at site 2+2a and site 3a+3b is shown. Note the strong correlation between the three variables. The Spearman rank correlation coefficient was calculated, and interdependency between the two variables was considered statistically significant if $p < 0.05$.

throughout muscle fibers (Fig. 4, *lower panel*). These observations are in agreement with our previous study in rabbit skeletal muscle, where the same specific intracellular distribution of P-GS1b and P-GS2+2a was observed (26).

Phosphorylation-dependent GS Association with Distinct Pools of Glycogen Particles—Control single muscle fibers were immunostained against P-GS1b or P-GS2+2a. The staining was detected with nano-gold and silver enhanced for transmission electron microscopy. Representative images of P-GS1b and P-GS2+2a distribution are shown in Fig. 5. The results show that both phospho-specific forms of GS are associated with glycogen particles, the diameter of which is ~25 nm (Fig. 5, *C* and *G*, *arrows*) agreeing with previously reported data (35, 36). The GS phospho-specific intracellular distribution responds to differential binding of GS with two pools of glycogen particles depending on its phosphorylation state. P-GS1b is mainly found associated with intramyofibrillar glycogen particles (Fig. 5, *A* and *B*), while P-GS2+2a is mainly associated with glycogen particles accumulated in the cytoplasm between the myofibrils, intermyofibrillar particles (Fig. 5, *D–F*). Note that immunolabeling against P-GS shows several silver enhanced nano-gold particles in each glycogen particle.

GS Intracellular Redistribution during Exhausting Exercise and at the Beginning of Glycogen Re-synthesis—GS intracellular distribution was investigated using fluorescence immunocytochemistry in single muscle fibers. In basal control fibers, GS presents a diffused pattern of distribution, particularly in the cross-striations and around the myonuclei (Fig. 6*A*). After exhausting exercise of control legs GS distribution changes from a diffuse to a more prominently striated pattern, indicating GS translocation to myofilaments in response to exhausting exercise (Fig. 6*B*). In exhausted pre-depleted muscle fibers, GS was found both in the striations as some spherical clusters and around myonuclei (Fig. 6*C*). Already before the exhausting exercise in some muscle fibers from pre-depleted muscle, which had been depleted of glycogen the day before and had been kept without glucose supply, GS was found associated with similar spherical clusters with a diameter of 200–500 nm. After exhausting exercise glycogen re-synthesis was investigated in pre-depleted legs. Thirty minutes after the end of exhausting exercise and the ingestion of a high glucose drink, GS was mainly detected associated with spherical particles at the striations of sarcomeres (Fig. 6*D*, *lower panel*).

DISCUSSION

Our results show that GS intrinsic activity is strongly associated with glycogen levels (Fig. 3*A*), supporting the hypothesis that GS is regulated through negative feedback by glycogen (37, 38). Furthermore, we show that GS activity in the presence of 0.02 mM or 0.17 mM G6P is strongly dependent on its phosphorylation state at sites 2+2a, 3a, and 3a+3b (Fig. 3*B*), and such phosphorylation states are in turn strongly dependent on muscle glycogen content (Fig. 3, *C* and *D*). Note that, in basal pre-depleted muscle, in which glycogen levels have been low overnight and are 49% of the level in basal control muscle, GS phosphorylation at sites 2+2a, 3a, and 3a+3b is significantly lower than in basal control legs (Fig. 2). This is in agreement with a previous study, which reported that GS phosphorylation at sites 3a and 2 is decreased in rested rat muscle with low glycogen levels (39, 40). Altogether our results indicate that GS

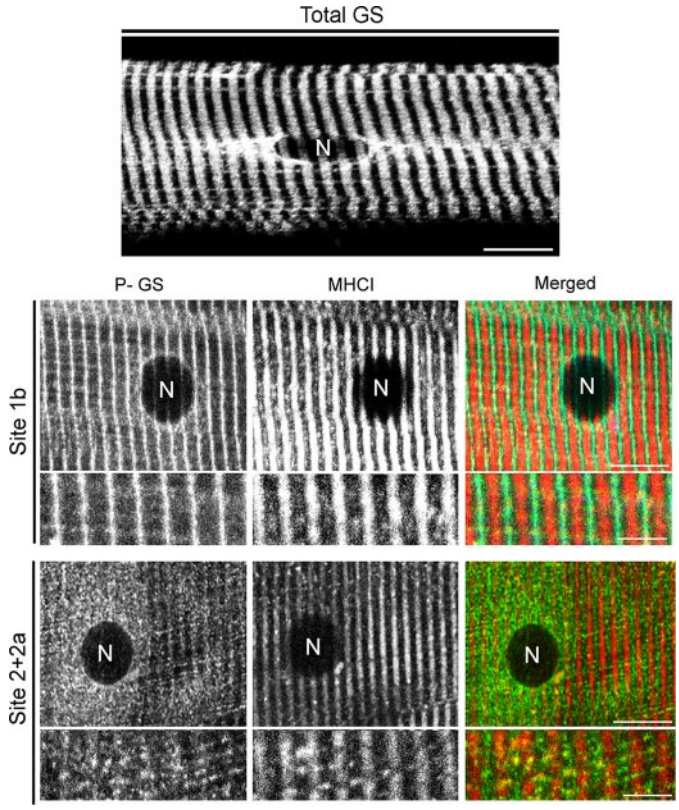

FIGURE 4. **Phosphorylation-dependent intracellular distribution of GS.** Single muscle fibers were obtained from vastus lateralis biopsies from six subjects at different time points. Immunostaining against total GS, GS phosphorylated at site 1b, or GS phosphorylated at site 2+2a was performed. Co-staining against myosin heavy chain type 1 (*MHCI*) was done to fiber type. *Top panel*, representative image of total GS intracellular distribution in a basal control muscle fiber is shown. *Bar* represents 10 μm. *Lower panel*, representative images of P-GS1b, P-GS2+2a, and MHCI distribution are shown. In both type I and II muscle fibers phosphorylated at site 1b, GS shows a striated pattern of distribution but, when phosphorylated at sites 2+2a, shows a dotted pattern of distribution. Note the presence of a lipofuscin granule (*LF*) next to the nucleus detected in the MHCI channel, *lower panel*. *Merged images* are shown in the *right-hand panel*. *Bars* represent 10 μm for the lower magnification images and 5 μm for the higher magnification images.

phosphorylation is strongly dependent on glycogen levels and that such regulation involves coordinate dephosphorylation of sites 2+2a, 3a, and 3a+3b (Fig. 3*D*). The regulatory mechanism by which glycogen content could regulate GS phosphorylation/dephosphorylation and intrinsic activity remains elusive. A recent study reports differential inhibitory properties of glycogen on AMPK activity depending on its branching degree (41), pointing toward AMPK as a potential mediator of the negative feedback of glycogen on GS activity. The phosphatase R_{GL}/G_MPP1 has been shown to play an essential role for muscle contraction-induced GS activation (42), but it is not known whether PP1 acts preferentially on specific GS sites.

Interestingly, even though phosphorylation of GS at sites 2+2a is strongly correlated with the enzyme activity in the presence of 0.17 and 0.02 mM G6P, dephosphorylated forms of GS at these sites can have a broad range of activity (Fig. 3*B*). In contrast, when dephosphorylated at sites 3a+3b, GS is highly active in the presence of 0.17 and 0.02 mM G6P. These results indicate that sites 3a and 3b are stronger regulators of GS intrinsic activity than sites 2+2a, because some samples had highly dephosphorylated GS at sites 2+2a but presented low activity.

Glycogen content in control legs after exhausting exercise and in basal pre-depleted legs were similar, but GS phosphorylation at sites 2+2a and 3a+3b were significantly decreased only after overnight low glycogen levels (Fig. 2). These observations indicate that the effect of glycogenolysis on GS phosphorylation is not immediate but time-dependent. Even though quite controversial, it has been proposed that *O*-linked *N*-acetylglucosamine modification of GS can inactivate the enzyme (43) by decreasing its susceptibility to GS phosphatases (44). If verified, one could speculate that overnight low glycogen levels could lead to enzymatic removal of *O*-linked *N*-acetylglucosamine modification of GS allowing phosphatases to completely dephosphorylate sites 2+2a and 3a+3b. This hypothesis is supported by a previous study (44), where GS from muscle with high glycogen levels was never fully activated in the absence of the phosphatase inhibitor sodium fluoride, indicating that something more than phosphorylation is down-regulating GS activity in muscle with high glycogen content but not in muscle with low glycogen content. Another possibility could be that exhausting exercise-induced activation of GS kinases, such as AMPK, PKA, calmodulin kinase II, or protein kinase C, could counteract glycogenolysis-induced GS dephosphorylation. This would explain the fact that only after certain rest time with low glycogen levels a significant decrease in GS phosphorylation at sites 3a+3b and 2+2a is detected. Furthermore, after overnight low glycogen levels, a clear decrease in GS phosphorylation at sites 2+2a was detected (Fig. 2). It has been shown that insulin stimulation leads to GS dephosphorylation at sites 2+2a and that such response is impaired in patients with T2DM and in women with polycystic ovary syndrome (5, 45). Considering that subjects after the glycogen depletion protocol on day 1 went home and had a low carbohydrate dinner, dephosphorylation of GS at sites 2+2a in pre-depleted muscle could respond to insulin stimulation during the postprandial state. Because limited glucose was available for GS to start glycogen re-synthesis, GS would remain activated on day 2 in basal pre-depleted muscle.

It is well known that GS phosphorylation sites mainly involved in the regulation of its intrinsic activity are sites 2+2a and 3a+3b (Fig. 3*B*) (22) and that sites 4 and 5 are linked to phosphorylation of site 3 (21). The question arises as to the role of GS phosphorylation at sites 1a and 1b. Analysis of interdependency between all phosphorylation sites and plasma insulin or epinephrine concentrations was performed, and only a statistically significant correlation between P-GS1b and epinephrine (correlation coefficient = 0.35, $p = 0.0075$) and insulin levels (correlation coefficient = -0.49, $p < 0.0005$) were detected. It is important to note that plasma insulin and epinephrine levels presented a strong negative correlation (correlation coefficient = -0.54, $p < 0.0005$). This correlation is mainly due to our experimental settings. Epinephrine levels increased during exhausting exercise and progressively decreased back to basal levels after 2-h rest, whereas insulin levels increased in response to the ingested high glucose drink and sandwich (Fig. 1, *left panel*). Considering that PKA is known to phosphorylate GS site 1b (46), and that after exhausting exercise an increase in site 1b phosphorylation was detected independent of glycogen levels (Fig. 2),

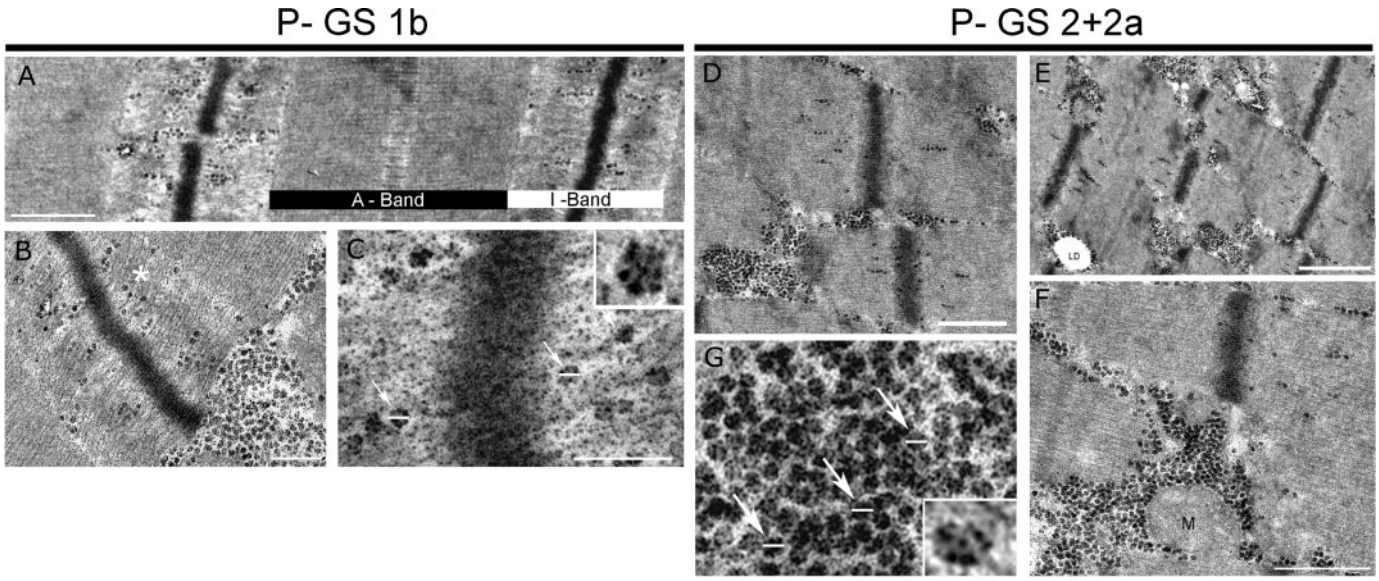

FIGURE 5. **Transmission electron microscopy analysis of P-GS1b and P-GS2+2a intracellular distribution.** Basal control biopsies were used to obtain single muscle fibers and perform nano-gold immunolabeling against P-GS1b (*A–C*) or P-GS2+2a (*D–G*). *A*, P-GS1b is mainly found at the A-band of the sarcomeres associated with actin filaments. *Bar* represents 0.5 μm. *B*, even though some P-GS1b is found associated with intermyofibrillar glycogen particles, most of it is associated with intramyofibrillar glycogen. *Bar* represents 200 nm. *C*, detail of P-GS1b positive glycogen particles. *Bar* represents 125 nm. Note that the diameter of the particles is around 25 nm (*arrows*), and there are several nano-gold silver-enhanced particles associated with each glycogen particle. *D–F*, P-GS2+2a is mainly found associated with the intermyofibrillar particles. *Bars* represent 500 nm in *D*, 1 μm in *E*, and 500 nm in *F*. Some can be found at the I-band of the sarcomeres, but in contrast to P-GS1b, it forms clusters. *G*, detail of P-GS2+2a-positive glycogen particles. Note that several P-GS2+2a are associated with each glycogen particle. Lipid droplet (*LD*) and mitochondrion (*M*).

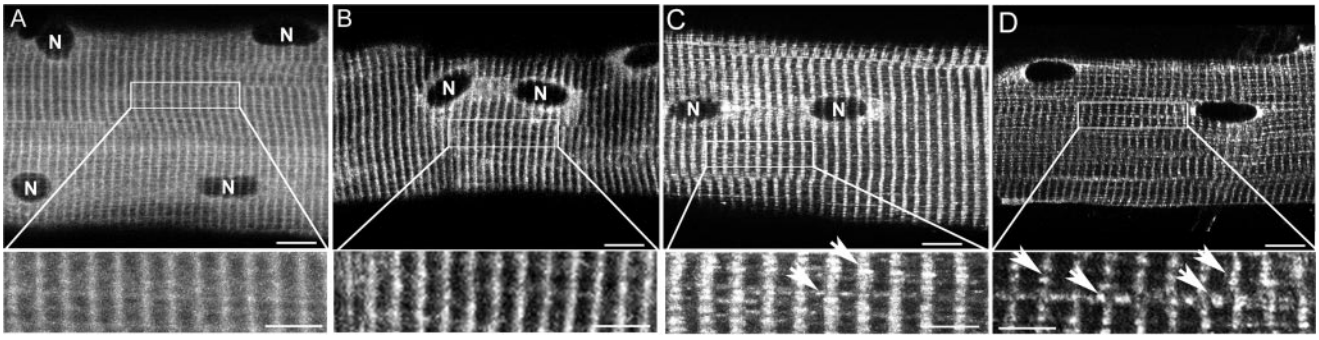

FIGURE 6. **GS intracellular redistribution during exhausting exercise and glycogen re-synthesis.** Single muscle fibers were obtained from vastus lateralis biopsies and used to analyses total GS intracellular distribution by fluorescence immunohistochemistry. Representative images of total GS intracellular distribution in a basal control muscle fiber (*A*), in a exhausted control muscle fiber (*B*), in a pre-depleted exhausted muscle fiber (*C*), and pre-depleted rested for 30 min muscle fiber (*D*) are shown. *Bars*, 12 μm. Details of the striation pattern at the different conditions are shown (*lower panel*). Note that GS distribution is more diffuse in basal control muscle fibers, whereas in both exhausted control or pre-depleted (*B* and *C*) muscle fibers GS is more concentrated at the A-band: the striations are easier to see. At the exhausted pre-depleted muscle fibers, clusters of GS start to appear, mainly located at the A-band of sarcomeres (*C*, *lower panel*: *arrows*). After 30-min rest, when glycogen re-synthesis is taking place, GS was found to form big clusters mainly at the A-band of sarcomeres (*D*, *lower panel*: *arrows*).

which coincides with the peak level of epinephrine in plasma (Fig. 1, *left panel*), our results indicate that, in response to exercise, epinephrine-induced PKA activation leads to muscle GS site 1b phosphorylation.

Furthermore, we show that P-GS1b is mainly found localized to the muscle cross-striations, specifically to the I-band of the sarcomeres (Fig. 4), while P-GS2+2a presents a dotted pattern of distribution. These observations support and extend our previous observations in rabbit skeletal muscle (26). To identify the exact cellular structures with which P-GS1b and P-GS2+2a associate, analysis of nano-gold immunocytochemistry by electron microscopy was performed. The results show that P-GS1b is mainly associated with glycogen particles located at the I-band, the so-called intramyofibrillar glycogen particles (Fig. 5). Skeletal muscle glycogen particles have been classified based on their intracellular location as subsarcolemmal, intra- or intermyofibrillar (47). All together, we report a mechanism of GS regulation based on intracellular compartmentalization. In response to exhausting exercise, elevated epinephrine plasma concentration leads to muscle PKA activation, which phosphorylates GS at site 1b targeting the enzyme to the intramyofibrillar glycogen particles.

Furthermore, electron microscopy analysis shows that P-GS2+2a is mainly associated with intermyofibrillar glycogen particles (Fig. 6), which form clusters of glycogen particles in between myofibrills, explaining the intracellular distribution observed by fluorescence immunocytochemistry (Fig. 4). The question arises: how does GS phosphorylation at different sites increase its affinity for a certain pool of glycogen particles? In addition, what is the difference between glycogen particles

located at the I-band of sarcomeres and glycogen particles found between the myofilaments?

Already in 1970 Meyer *et al.* (36) observed that different proteins were associated with glycogen particles and compared glycogen particles with cellular organelles. Twenty-six years later, Rybicka (48) described glycogen particles as independent metabolic units with specialized functions, glycosomes. Today it is well known that several proteins can associate to glycogen particles and that glycogen proteome is not static but can change depending on metabolic needs (see Ref. 49 for review).

Different pools of glycogen particles do not respond equally to exercise. Sustained submaximal exercise leads to glycogen depletion of the subsarcolemmal and intermyofibrillar pools of glycogen (50), whereas glycogen particles associated with sarcoplasmic reticulum are more sensitive to muscle contraction-induced glycogenolysis (36, 51–53). Thus, glycogen metabolism is complexly regulated by intracellular compartmentalization, and different glycogen pools are probably used for different cellular functions. Our results show that GS association with different glycogen pools is phosphorylation-dependent and that exhausting exercise leads to an increase in P-GS1b, which is associated with the intramyofibrillar glycogen particles (Figs. 2, 4, and 5). Note that GS associated with the intramyofibrillar glycogen particles is weakly immunodetected by the phospho-specific antibody against P-GS2+2a, indicating that it is dephosphorylated at such sites and is therefore more active. This could translate into a higher glycogen re-synthesis after exhausting exercise in the intramyofibrillar particles, which are preferentially used during muscle contraction (2–5). Further studies are needed to fully understand the physical binding of the different phosphorylation forms of GS to specific glycogen pools and the functional implications on muscle glycogen metabolism.

Changes in glycogen content occur as a result of the net balance between GS and phosphorylase activities. To fully understand glycogen metabolism in response to exhausting exercise, phosphorylase activity and its intracellular distribution should also be investigated.

Electron microscopy analysis of basal muscle immunolabeled against P-GS1b and P-GS2+2a (Fig. 5) show several silver-enhanced nano-gold particles associated with each glycogen particle. There has been and still is an ongoing discussion with regard to the number of GS molecules that can be associated with one particle of glycogen. Our results show that more than one GS molecule can be associated with each glycogen particle (Fig. 5, *C* and *G*).

In a previous study (26), using electrical stimulation of rabbit tibialis anterior muscle, we reported a novel cellular compartment involved in glycogen re-synthesis. After strong glycogen depletion, actin cytoskeleton rearrangement forms some spherical structures at the A-band of the sarcomeres to which glycogen enzymes gather at the start of glycogen re-synthesis. One of the aims of the present study was to investigate the existence of such novel cellular compartments in human skeletal muscle during physiological conditions. Our results show the formation of such spherical structures already in the basal pre-depleted leg (Fig. 6*C*), and these become more abundant and frequent after 30- and 120-min rest in pre-depleted exhausted muscle (Fig. 6*D*). These results support an emerging concept in cellular metabolism. Dynamic cellular compartments are formed in response to certain metabolic situations, probably to assemble the needed enzymes and cofactors and increase the efficiency of the metabolic processes. Further studies are underway to investigate when, what, how, and how long. When are these structures needed? What are the signals that induce their formation? How are these structures formed? How long do they last?

Acknowledgments—We thank Prof. Grahame D. Hardie (Division of Molecular Physiology, University of Dundee, Dundee, Scotland), Prof. Oluf Pedersen (Steno Diabetes Center, Denmark), and Prof. Joan J. Guinovart (Dept. of Biochemistry and Molecular Biology, University of Barcelona, Spain) for donating materials essential to this study, and acknowledge Betina Bolmgren and Jeppe Bach for skilled technical assistance.

REFERENCES

1. Bogardus, C., Lillioja, S., Stone, K., and Mott, D. (1984) *J. Clin. Invest.* **73,** 1185–1190
2. Roden, M., Petersen, K. F., and Shulman, G. I. (2001) *Recent Prog. Horm. Res.* **56,** 219–237
3. Shulman, G. I., Rothman, D. L., Jue, T., Stein, P., DeFronzo, R. A., and Shulman, R. G. (1990) *N. Engl. J. Med.* **322,** 223–228
4. Damsbo, P., Vaag, A., Hother-Nielsen, O., and Beck-Nielsen, H. (1991) *Diabetologia* **34,** 239–245
5. Højlund, K., Staehr, P., Hansen, B. F., Green, K. A., Hardie, D. G., Richter, E. A., Beck-Nielsen, H., and Wojtaszewski, J. F. (2003) *Diabetes* **52,** 1393–1402
6. Højlund, K., and Beck-Nielsen, H. (2006) *Curr. Diabetes Rev.* **2,** 375–395
7. Schalin-Jäntti, C., Härkonen, M., and Groop, L. C. (1992) *Diabetes* **41,** 598–604
8. Eriksson, J., Franssila-Kallunki, A., Ekstrand, A., Saloranta, C., Widén, E., Schalin, C., and Groop, L. (1989) *N. Engl. J. Med.* **321,** 337–343
9. Vaag, A., Henriksen, J. E., and Beck-Nielsen, H. (1992) *J. Clin. Invest.* **89,** 782–788
10. Roach, P. J. (1991) *J. Biol. Chem.* **266,** 14139–14142
11. Rothman-Denes, L. B., and Cabib, E. (1971) *Biochemistry* **10,** 1236–1242
12. Villar-Palasi, C. (1991) *Biochim. Biophys. Acta* **1095,** 261–267
13. Flotow, H., and Roach, P. J. (1989) *J. Biol. Chem.* **264,** 9126–9128
14. Flotow, H., Graves, P. R., Wang, A. Q., Fiol, C. J., Roeske, R. W., and Roach, P. J. (1990) *J. Biol. Chem.* **265,** 14264–14269
15. Carling, D., and Hardie, D. G. (1989) *Biochim. Biophys. Acta* **1012,** 81–86
16. Huang, T. S., and Krebs, E. G. (1977) *Biochem. Biophys. Res. Commun.* **75,** 643–650
17. Roach, P. J., DePaoli-Roach, A. A., and Larner, J. (1978) *J. Cyclic Nucleotide. Res.* **4,** 245–257
18. DePaoli-Roach, A. A., Ahmad, Z., Camici, M., Lawrence, J. C., Jr., and Roach, P. J. (1983) *J. Biol. Chem.* **258,** 10702–10709
19. Fiol, C. J., Mahrenholz, A. M., Wang, Y., Roeske, R. W., and Roach, P. J. (1987) *J. Biol. Chem.* **262,** 14042–14048
20. Picton, C., Woodgett, J., Hemmings, B., and Cohen, P. (1982) *FEBS Lett.* **150,** 191–196
21. Roach, P. J. (1990) *FASEB J.* **4,** 2961–2968
22. Skurat, A. V., Wang, Y., and Roach, P. J. (1994) *J. Biol. Chem.* **269,** 25534–25542
23. Villar-Palasi, C. (1995) *Biochim. Biophys. Acta* **1244,** 203–208
24. Fernández-Novell, J. M., Bellido, D., Vilaró, S., and Guinovart, J. J. (1997) *Biochem. J.* **321,** 227–231
25. Ferrer, J. C., Baqué, S., and Guinovart, J. J. (1997) *FEBS Lett.* **415,** 249–252
26. Prats, C., Cadefau, J. A., Cussó, R., Qvortrup, K., Nielsen, J. N., Wojtaszewki, J. F., Wojtaszewki, J. F., Hardie, D. G., Stewart, G., Hansen, B. F., and

Ploug, T. (2005) *J. Biol. Chem.* **280,** 23165–23172
27. Andersen, P., Adams, R. P., Sjøgaard, G., Thorboe, A., and Saltin, B. (1985) *J. Appl. Physiol.* **59,** 1647–1653
28. Bergström, J. (1962) *Scand. J. Clin. Lab. Invest.* **14,** Suppl. **68,** 11–13
29. Stefanini, M., De Martino, C., and Zamboni, L. (1967) *Nature* **216,** 173–174
30. Ploug, T., van Deurs, B., Ai, H., Cushman, S. W., and Ralston, E. (1998) *J. Cell Biol.* **142,** 1429–1446
31. Prats, C., Bernal, C., Cadefau, J. A., Frias, J., Tibolla, M., and Cusso, R. (2002) *Biochim. Biophys. Acta* **1573,** 68–74
32. Højlund, K., Glintborg, D., Andersen, N. R., Birk, J. B., Treebak, J. T., Frøsig, C., Beck-Nielsen, H., and Wojtaszewski, J. F. (2008) *Diabetes* **57,** 357–366
33. Höjlund, K., Staehr, P., Hansen, B. F., Green, K. A., Hardie, D. G., Richter, E. A., Beck-Nielsen, H., and Wojtaszewski, J. F. P. (2003) *Diabetes* **52,** 1393–13402
34. Dawson, D. J., and Nichol, L. W. (1969) *Aust. J. Biol. Sci.* **22,** 247–255
35. Marchand, I., Chorneyko, K., Tarnopolsky, M., Hamilton, S., Shearer, J., Potvin, J., and Graham, T. E. (2002) *J. Appl. Physiol.* **93,** 1598–1607
36. Meyer, F., Heilmeyer, L. M., Jr., Haschke, R. H., and Fischer, E. H. (1970) *J. Biol. Chem.* **245,** 6642–6648
37. Danforth, W. H. (1965) *J. Biol. Chem.* **240,** 588–593
38. Nielsen, J. N., Derave, W., Kristiansen, S., Ralston, E., Ploug, T., and Richter, E. A. (2001) *J. Physiol.* **531,** 757–769
39. Jørgensen, S. B., Nielsen, J. N., Birk, J. B., Olsen, G. S., Viollet, B., Andreelli, F., Schjerling, P., Vaulont, S., Hardie, D. G., Hansen, B. F., Richter, E. A., and Wojtaszewski, J. F. (2004) *Diabetes* **53,** 3074–3081
40. Lai, Y. C., Stuenaes, J. T., Kuo, C. H., and Jensen, J. (2007) *Am. J. Physiol. Endocrinol. Metab.* **293,** E1622–1629
41. McBride, A., Ghilagaber, S., Nikolaev, A., and Hardie, D. G. (2009) *Cell Metab.* **9,** 23–34
42. Aschenbach, W. G., Suzuki, Y., Breeden, K., Prats, C., Hirshman, M. F., Dufresne, S. D., Sakamoto, K., Vilardo, P. G., Steele, M., Kim, J. H., Jing, S. L., Goodyear, L. J., and DePaoli-Roach, A. A. (2001) *J. Biol. Chem.* **276,** 39959–39967
43. Parker, G. J., Lund, K. C., Taylor, R. P., and McClain, D. A. (2003) *J. Biol. Chem.* **278,** 10022–10027
44. Wojtaszewski, J. F., Jørgensen, S. B., Hellsten, Y., Hardie, D. G., and Richter, E. A. (2002) *Diabetes* **51,** 284–292
45. Glintborg, D., Højlund, K., Andersen, N. R., Hansen, B. F., Beck-Nielsen, H., and Wojtaszewski, J. F. (2008) *J. Clin. Endocrinol. Metab.* **93,** 3618–3626
46. Cohen, P., Alessi, D. R., and Cross, D. A. (1997) *FEBS Lett.* **410,** 3–10
47. Fridén, J., Seger, J., and Ekblom, B. (1989) *Acta Physiol. Scand.* **135,** 381–391
48. Rybicka, K. K. (1996) *Tissue Cell* **28,** 253–265
49. Roach, P. J., Cheng, C., Huang, D., Lin, A., Mu, J., Skurat, A. V., Wilson, W., and Zhai, L. (1998) *J. Basic Clin. Physiol. Pharmacol.* **9,** 139–151
50. Sjöström, M., Fridén, J., and Ekblom, B. (1982) *Histochemistry* **76,** 425–438
51. Goldstein, M. A., Murphy, D. L., van Winkle, W. B., and Entman, M. L. (1985) *J. Muscle Res. Cell Motil.* **6,** 177–187
52. Wanson, J. C., and Drochmans, P. (1968) *J. Cell Biol.* **38,** 130–150
53. Wanson, J. C., and Drochmans, P. (1972) *J. Cell Biol.* **54,** 206–224